Characterization of Angiogenesis Assays to Probe Metabolic Profiles of Tip and Stalk Cells

By

Lindsey Nicole Sabo

Thesis

Submitted to the Faculty of the

Graduate School of Vanderbilt University

in partial fulfillment of the requirements

for the degree of

MASTER OF SCIENCE

in

Biomedical Engineering

May 10, 2024

Nashville, Tennessee

Approved:

Dr. Cynthia Reinhart-King, Ph.D.

Dr. Marc Moore, Ph.D.

ACKNOWLEDGMENTS

I would like to thank Dr. Reinhart-King for all the guidance and support over the past two years. I was an undergraduate with no research or lab experience when I requested to join her lab, and Dr. Reinhart-King was willing to provide me with the experience I needed. Dr. Reinhart-King helped me many times to overcome obstacles to progress with her insightful thoughts. Dr. Reinhart-King has been a great advisor, and I grew a lot during my time working with her.

I would like to thank all the members of the Reinhart-King Lab for all their help and support throughout my time at Vanderbilt University. I would like to especially thank Dr. Paul Taufalele. He taught me almost everything I know about lab work and research, and I definitely would not be where I am today without him.

I would like to thank my family and friends for their continual support of my academic career. They were always there for me when I was overwhelmed and helped me to keep moving forward.

TABLE OF CONTENTS

Page

LIST OF FIGURES

Page

Chapter 1

Introduction

1.1 Introduction to Angiogenesis

Angiogenesis is the generation of new blood vessels from existing vasculature and is essential for growth and development of the human body [1]. All metabolically active tissues are within a few hundred microns of a capillary to ensure sufficient nutrient and oxygen delivery [2]. There are two types of angiogenesis that occur both in utero and throughout life: intussusceptive and sprouting. Intussusceptive angiogenesis occurs when an existing blood vessel splits into two vessels without requiring immediate endothelial cell proliferation or migration and primarily occurs during embryo development [2]. Sprouting angiogenesis occurs when endothelial cells diverge from the exterior of an existing blood vessel and migrate toward an angiogenic stimulus [2]. In many cases, the angiogenic stimulus is the vascular endothelial growth factor VEGF-A that is secreted from poorly perfused tissues as a result of hypoxic conditions [3]. Sprouting angiogenesis consists of several steps: enzymatic degradation of the capillary basement membrane and the extracellular matrix, endothelial cell proliferation, directed migration, and lumen formation [3]. Sprouting angiogenesis is a fundamental process in developmental biology, but it also can act as a pathological event that initiates or aggravates various disease states [4]. Because of this, sprouting angiogenesis is the focus of this study.

1.2 Physiological Significance

Angiogenesis plays an important role in many crucial physiological processes. For example, neovascularization is a critical element of wound healing. Uninjured tissues are adequately vascularized for sufficient nutrient and oxygen delivery, as well as removal of waste products and carbon dioxide. However, when an injury occurs, the native vasculature is disrupted, resulting in fluid accumulation, inflammation, and the development of hypoxia [5]. Hypoxic conditions activate the transcription factor hypoxia-inducible factor-1-alpha (HIF-1α) and promote production of pro-angiogenic growth factors such as VEGF-A, Ang-2, and SDF-1 [6]. The resulting angiogenic activity creates a dense, disordered vascular network with many dead-end flow pathways and high tortuosity [6]. After this initial network has formed, anti-angiogenic

growth factors induce regression of the vascular network to reduce the abnormally high vessel density [6, 7]. This is followed by vessel maturation via recruitment of smooth muscle cells and pericytes to stabilize the vascular architecture [6, 7]. The disrupted vasculature is now restored to a non-hypoxic state and the injured tissue is adequately perfused as a result of angiogenesis.

Angiogenesis also plays a key role in cancer progression. A study conducted in 1982 by Muthukkaruppan and colleagues found that tumor cells were unable to grow beyond 2 mm^3 without vascular support [8]. Another study found that tumors may become necrotic or apoptotic when vascularization is prevented [9]. Because of uncontrolled cell proliferation and altered metabolism, developing tumors experience inadequate transport of nutrients and oxygen and enter a hypoxic state [10, 11]. When this occurs, tumors secrete a variety of angiogenic growth factors (most commonly VEGF and bFGF) that bind tyrosine kinase receptors on the membranes of endothelial cells [11]. This triggers a variety of signaling cascades, including the mitogen activated protein kinase (MAPK) pathway, that activates and translocates the appropriate transcription factors into the nucleus to stimulate neovascularization [11]. Nutrient and oxygen transport to the tumors subsequently improve, allowing them to continue to grow [11, 12]. This demonstrates the importance of angiogenesis for cancer progression and shows that prevention of tumor-induced neovascularization could act as a cancer therapy.

Another important application of angiogenesis is tissue engineering. Tissue engineering is the practice of combining scaffolds, cells, and biologically active molecules into functional tissues that restore, maintain, or improve damage to native tissues or organs [13]. While many studies have demonstrated the therapeutic potential of tissue replacement with tissue engineered constructs, there are very few clinical applications [14]. One of the main reasons for this is the difficulty of incorporating mature and functional vasculature into the constructs. Without sufficient vascular ingrowth, necrosis will occur within the scaffold and potentially cause transplant rejection [14, 15]. Additionally, it has been noted that the size and complexity of many tissue engineered products are limited by the lack of blood vessel networks [16]. Developing a better understanding of angiogenesis and its underlying mechanisms is therefore crucial to create advanced tissue engineered constructs that have the potential for clinical application.

1.3 Common Platforms for Study

There are many different methods to model and subsequently study angiogenesis. One of the most common models is the spheroid sprouting assay. This assay consists of self-aggregated

endothelial cells embedded in a 3D matrix that sprout and invade their surroundings when stimulated with relevant growth factors [17]. The 3D matrix composition is typically collagen, fibrin, or another common component of the extracellular matrix. This assay replicates the formation of capillaries from existing vessels with high accuracy [17]. Because this model incorporates a 3D matrix, it promotes endothelial cell-cell signaling and mimics the *in vivo* environment better than older 2D models [18]. Additionally, the simplicity of this model allows for rapid investigation of various properties of angiogenesis.

Another method to model angiogenesis is a microcarrier-based assay. This assay is very similar to the spheroid sprouting assay. Microcarriers are small beads that encourage cell attachment and are commonly made of materials like gelatin, dextran, cellulose, plastic, or glass [19]. Endothelial cells adhered to microbeads are embedded in a 3D matrix and allowed to sprout and invade [20]. This assay offers the same advantages as the spheroid sprouting assay.

The aortic ring assay is another platform to study angiogenesis. This assay is considered to be in between *in vitro* and *in vivo* study. To generate this model, a mouse or rat thoracic aorta is excised, sliced into thin rings, and embedded in a 3D matrix [21]. Because the aorta does not include solely endothelial cells, the resulting outgrowths are able to recruit surrounding smooth muscle cells and pericytes to the newly forming vessels [22]. This results in a model with high anatomical accuracy relative to *in vivo* neovessels. A disadvantage of this model is that angiogenic outgrowths *in vivo* occur from microvessels, not from major vessels like the aorta [21]. This suggests that the neovascularization observed from this assay could have slight differences from *in vivo* neovascularization. Additionally, aortic rings from mice of different ages or strains could have inconsistent angiogenic responses [21]. However, the anatomical similarity of the newly generated vessels makes this model a valuable tool for investigation of angiogenesis.

Angiogenesis is also commonly investigated using the *in vivo* model of a chick chorioallantoic membrane (CAM) assay. The CAM is an extraembryonic membrane that serves as a surface for gas exchange and is supported by a dense capillary network [23]. Its extensive vascularization and accessibility allow for the study of morphofunctional aspects of angiogenesis, as well as the mechanisms of action of proangiogenic and antiangiogenic molecules [23]. The CAM assay is relatively inexpensive, and it can be adapted to a variety of applications, such as assessments of inflammation, tumor, or cytokine-induced angiogenesis [24].

1.4 Known Mechanisms of Action

1.4.1 Tip vs Stalk Differentiation

During sprouting angiogenesis, endothelial cells acquire two distinct cellular phenotypes: tip cells and stalk cells. Both cell types are essential for the generation of a new, mature vascular network. Tip cells are found at the extremity of a budding sprout and guide the subsequent angiogenic outgrowth [25]. They are characterized by their migratory behavior and dynamic filopodia that probe the extracellular environment [26]. Vascular endothelial growth factor receptor 2 (VEGFR2), which binds VEGF-A, is upregulated in tip cells and primarily localizes to the filopodia [27]. This allows tip cells to effectively sense the direction of an existing VEGF-A gradient and lead the sprout toward the source. Stalk cells, on the other hand, follow the tip cell and support sprout elongation and nascent lumen formation [26]. They are characterized by high levels of proliferation and secure cell-cell adhesions via tight junctions to ensure sprout stability [26].

The phenotype of an endothelial cell during sprouting is dynamic, regulated by the VEGF and Notch signaling pathways (Figure 1). When VEGF-A binds to its receptor VEGFR2 on an endothelial cell, expression of Dll4, a membrane ligand of the Notch1 receptor, is upregulated [28]. Dll4 binds to Notch receptors on adjacent endothelial cells, resulting in proteolytic release of the Notch intracellular domain (NICD) [28, 29]. NICD release results in lower expression of VEGFR2 in the adjacent endothelial cells [29]. Without high levels of VEGFR2, these cells are unable to sense or interact with VEGF-A and acquire the stalk cell phenotype. Stalk cells have increased levels of Jagged-1, another membrane Notch ligand, that antagonizes Dll4/Notch signaling and therefore encourages tip cells to maintain their phenotype without the influence of NICD [28]. In this way, endothelial cell phenotype is a result of various feedback loops from the interactions of VEGF and Notch signaling. The most “competitive” endothelial cell, or the cell that is best fit to lead the sprout, takes on the role of the tip cell. Endothelial cells are constantly switching phenotypes and competing for the leading position as lateral inhibition varies as a result of the feedback loops [29].

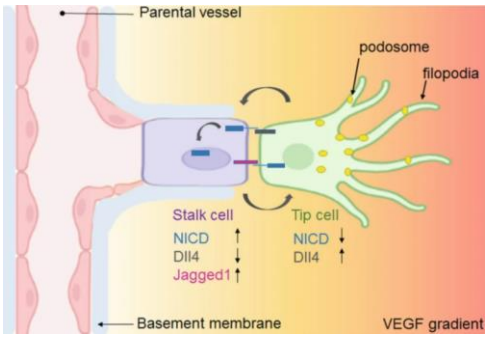

Figure 1. Visual representation of regulation of endothelial cell phenotype during angiogenesis through Notch signaling and lateral inhibition. From Dong, *et al.* 2023.

1.4.2 Matrix Metalloproteinases for ECM Degradation

In order for endothelial cells to migrate and invade surrounding tissues, degradation of the vascular basement membrane and remodeling of the extracellular matrix (ECM) is required [3, 30]. To accomplish this, a class of enzymes called matrix metalloproteinases are upregulated on endothelial tip cells [26, 31]. Matrix metalloproteinases, or MMPs, proteolytically degrade components of the ECM [30]. One of the most studied MMPs that participates in angiogenesis is MMP-14 (also known as MT1-MMP). MMP-14 is a transmembrane protein that can degrade a variety of ECM components, including collagen (I, II, III), gelatin, fibronectin, laminin, aggrecan, and tenascin [32, 33]. MMP-14 is also thought to contribute to the progression of angiogenesis by playing a role in endothelial cell migration, vessel maturation, and modulation of MMP-2, a gelatinase that is simultaneously expressed on endothelial tip cells [33, 34].

1.4.3 Effects of Matrix Density

As previously stated, the formation of new vasculature involves endothelial cell migration through the extracellular matrix. It has been previously demonstrated that mechanical interactions between angiogenic sprouts and the ECM impact the overall vascular architecture in a variety of ways [35-37]. One important mechanism by which the ECM influences angiogenesis is through matrix density, or stiffness. Various studies have shown that increased ECM density leads to reduced angiogenesis and decreased ECM density leads to increased angiogenesis [37-40]. This is thought to occur because stiffer matrices limit the generation of cellular actomyosin contractions that are required for cell migration [39, 40].

1.4.4 Metabolism

Cell metabolism is the catabolic process by which cells convert nutrients into energy and is required for angiogenic growth [41, 42]. In addition to providing the required energy for neovascularization (cell migration, cell proliferation, and matrix degradation), it has been demonstrated that endothelial cell metabolism is a key determinant of the differentiation and functioning of the distinct endothelial cell phenotypes [43-45]. One of the most important metabolic pathways that contributes to and regulates endothelial cell phenotype during angiogenesis is glycolysis. Glycolysis has been shown to generate up to 85% of the total ATP content in endothelial cells, suggesting that it is the predominant bioenergetic pathway for angiogenesis [45]. Because oxygen levels decrease more rapidly than glucose levels as the distance from perfused blood vessels increases, glycolysis is an ideal metabolic pathway for angiogenesis [46].

In endothelial tip cells, upregulation of enzymes such as PFKFB3 and PFK1 increases glycolytic ATP generation [44, 45]. These enzymes form a functional "assembly line" along F-actin fibers to allow for incredibly efficient ATP production and utilization [47]. The majority of the ATP generated from this process localizes to regions of active cytoskeletal remodeling, such as the filipodia and lamellipodia, to drive cell migration [48]. Tip cell metabolism increases in environments where migration and invasion are more challenging, such as denser matrices [49]. Endothelial stalk cells also exhibit high levels of glycolytic activity to sustain rapid cell proliferation [44]. In addition to ATP, glycolysis produces acetyl-CoA, which can enter the TCA cycle to generate ribonucleoside triphosphates (rNTPs) and deoxynucleotide triphosphates (dNTPs) that support the quick RNA and DNA synthesis that accompanies rapid cell division [44]. However, the NICD has been shown to reduce glycolytic rates by inhibiting the activity of enzymes like PFKFB3 [50]. Because the NICD is an active transcription factor in stalk cells due to increased Notch signaling, this results in a decrease in glycolytic activity relative to tip cells [50, 51].

1.5 Thesis Objectives

As a result of the innate similarities between the *in vitro* spheroid and microbead models of angiogenesis, these assays needed to be characterized and compared, as the subtle differences in their angiogenic features that could inform one's decision of which angiogenic model to use based on the investigative needs. Additionally, it has been previously reported that angiogenesis is highly dependent on the physical properties of the ECM. However, the specific impact of the

ECM on the metabolism of the stalk endothelial subtype is not well known. Furthermore, the potential role of stalk cells in matrix degradation has been poorly investigated. We hypothesized that collagen density, which impacts matrix stiffness and pore size, directly affects the glycolytic metabolism of endothelial cells undergoing angiogenesis, with a more pronounced effect on tip cells as compared to stalk cells. We further hypothesized that the ability to facilitate matrix degradation through functional MMP-14 is not required for stalk cell differentiation. To address these hypotheses, we developed three aims:

1. Characterize and compare the spheroid and microbead assays of angiogenesis and identify the optimal model for subsequent analysis.
2. Investigate the effects of collagen density on metabolic activity of stalk cells along angiogenic sprouts.
3. Generate a HUVEC cell line with an MMP-14 KO for future analysis of the role of MMP-14 in tip and stalk endothelial cells.

When the two assays were compared, we found that the spheroid assay generated increased angiogenic output relative to the microbead assay. We chose to use the spheroid assay for future analyses because of this advantage. Investigation of the effects of collagen density on stalk cell metabolic activity suggested that stalk cells may have an ability to adapt their metabolism in response to matrix changes. Attempts to generate a HUVEC line with an MMP-14 KO with exponential decay electroporation resulted in cell death and were therefore unsuccessful. Future attempts will include altered electroporation settings and chemical transfection with lipofectamine.

Chapter 2
Methods

2.1 Cell Culture and Reagents

Human umbilical vein endothelial cells (HUVECs) were cultured with endothelial growth medium 2 (EGM-2) from Lonza and incubated at 37 °C and 5% CO_2. EGM-2 includes several growth factors, including hFGF-B, VEGF, R3-IGF-1, and hEGF. HUVECs were seeded into cell culture flasks at densities of 150k cells (T25) or 450k cells (T75) and the media was changed every other day. HUVECs were cultured until around 70% confluent and then passaged. HUVECs were maintained until their fifth passage.

2.2 Microbead Generation

Cytodex-3 microcarriers (Cytivia) were hydrated in 5 ml PBS overnight. They were then sterilized with a 30 minute liquid autoclave cycle at 121 °C and allowed to cool off for 30 minutes. The microcarriers were washed two times with 5 ml sterile PBS and placed in a 15 ml tube with 5 ml EGM-2. The desired number of cells were added to the solution to create cell to bead ratios of 5:1. 50:1, or 200:1. They were incubated at 37 °C and 5% CO_2 for four hours on an orbital shaker at approximately 2 rev/s. The microbead/cell solution was then transferred to a T25 flask and incubated for sixteen hours on the orbital shaker, still at 2 rev/s.

2.3 Spheroid Generation

Approximately 1200 HUVECs in 0.25% Methocult were added to each well of a sterile, U bottom 96 well plate to create 1.2k cell spheroids. The 96 well plate was centrifuged at 1100 RPM for five minutes. If the cells did not appear to be sufficiently aggregated at the bottom of each well, the plate was centrifuged again for five minutes. The spheroids were incubated at 37 °C and 5% CO_2 for 24 hours.

2.4 Embedding in Collagen

Collagen solutions were prepared at densities of 1.5, 3, or 4.5 mg/ml in 0.1% acetic acid and neutralized with HEPES buffer. After spheroids or microbeads were placed in the collagen solution, 1 N NaOH was added and the solution was mixed until homogenous. Approximately 3-5 spheroids in 40 µl collagen solution were placed in four wells of a 24 well glass plate. For microbeads, 500 µl collagen solution was placed in two wells of a 24 well plate. The solutions were allowed to polymerize for 40-45 minutes before 1 ml EGM-2 was placed on top of each well. The gels were incubated for 24 hours at 37 °C and 5% CO_2 to allow for growth before fixing, staining, and imaging.

2.5 Glucose Uptake Assay

Glucose uptake was measured using the fluorescent glucose analog 2-NBDG (Invitrogen). After 24 hours of incubation, the media for each collagen gel was replaced with 0.146 mM 2-NBDG in EGM-2. The gels were fixed and imaged after an additional 24-hour incubation at 37 °C and 5% CO_2.

2.6 Fixing and Staining

After 24 hours of incubation, collagen gels with spheroids or microbeads were washed two times with PBS and incubated with 1 ml/gel 3.2% paraformaldehyde at room temperature for 15 minutes. The gels were subsequently washed three times with PBS for 5 minutes. The gels were then permeabilized with 1 ml/well 1% Triton-X and incubated for one hour at room temperature on a rocker. Each well was then washed three times for twenty minutes with 0.02% Tween 20 in PBS. To create the staining solution, TexasRed-X Phalloidin (ThermoFisher) was diluted 1:50 and DAPI (Sigma) was diluted 1:300 in 0.02% Tween 20. 100 µl of this solution was placed on top of each gel and stored overnight on a rocker at 4 °C. Prior to imaging, the gels were washed twice for ten minutes with 0.02% Tween 20 and PBS.

2.7 Fluorescent Microscopy

TexasRed-X Phalloidin, DAPI, and 2-NBDG were measured on an LSM700 confocal microscope using a 20x water immersion objective. TexasRed-X Phalloidin was excited using a 555 nm laser, DAPI was excited using a 405 nm laser, and 2-NBDG was excited using a 488 nm laser. All images were quantified using ImageJ.

2.8 Electroporation/Transfection of HUVECs with MMP14 KO sgRNA

A CRISPR/cas9 KO kit from Synthego was used for transfection. RNP complexes were formed with a 9:1 ratio of sgRNA and cas9. The RNP complex were added to $1x10^6$ HUVECs in 200 µl electroporation buffer. The solution was subjected to an exponential decay pulse at 120 V and 950 µF. Immediately after electroporation, the cells were transferred to a T25 flask with 5 ml of pre-warmed EGM-2 and incubated at 37 °C and 5% CO_2.

Chapter 3
Results

As previously described, the most common *in vitro* models used to study angiogenesis are the spheroid and microbead assays. These models both replicate the formation of capillaries from existing vessels with high accuracy, promote endothelial cell-cell signaling, and mimic the *in vivo* environment better than older 2D models. Additionally, the simplicity of these models allows for

rapid investigation of various properties of angiogenesis. In order to select the optimal assay for investigation of the metabolic profiles of tip and stalk cells during sprouting angiogenesis in 3D matrices, these models were characterized and compared. We found that the spheroid assay resulted in increased angiogenic output when compared to the microbead assay. We chose to use the spheroid assay for our subsequent analysis because of this advantage.

Next, we investigated the effects of collagen density on the metabolic activity of stalk cells during angiogenesis. Denser matrices pose a larger barrier to cell migration and therefore increase the energy requirement for angiogenesis. Tip cells are the main drivers of cell migration and demonstrate increased metabolic activity in environments where invasion is more challenging, such as denser matrices. On the other hand, stalk cells have not been shown to play a large role in cell migration, so we hypothesized that their metabolism would not adapt to help with the increased energetic burden that results from increased matrix densities. Interestingly, we found that as collagen density increased, there was no significant difference in tip-stalk metabolic activity.

We then attempted to generate a HUVEC line with an MMP-14 KO using electroporation with an exponential decay pulse. This resulted in cell death during the recovery phase and was therefore unsuccessful. Future attempts will include altered electroporation settings and chemical transfection with lipofectamine.

3.1 Microbead Assay Optimization using Cytodex-3 Microcarriers

Generation of the microbead assay for investigation of angiogenesis is somewhat inconsistent across literature, so an optimized protocol had to first be determined. Cytodex-3 microcarriers were used for this assay. These microcarriers consist of a thin layer of denatured collagen coupled to a matrix of crosslinked dextran and were designed for the culture of primary cells [52].

The primary difference in microbead generation in literature is the ratio of HUVECs to microbeads. This ratio varies from as low as 11 cells/bead to as high as 400 cells/bead [53-56]. To determine an effective cell to bead ratio, HUVECs were incubated with the microbeads at ratios of 5:1, 50:1, and 200:1, and the level of cell attachment to the beads was observed. The 5:1 cell to bead ratio resulted in microbeads that were only partially covered with cells, while the 50:1 cell to bead ratio resulted in complete coverage (Figure 2A, B). The 200:1 cell to bead ratio also resulted in complete coverage of the microbeads, but it showed excessive cell aggregation on the surface of the microcarriers that led to clumping (Figure 2C, D). Because clumping of the microbeads

would interfere with angiogenic growth, the 50:1 cell to bead ratio was selected as optimal and used for subsequent experiments.

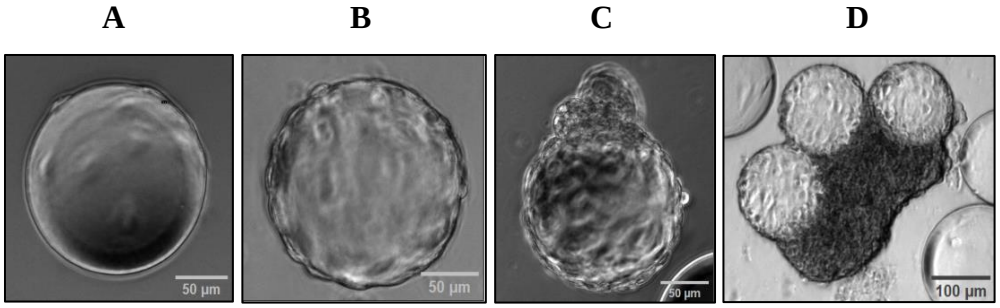

Figure 2. Representative images of the degree of HUVEC attachment to Cytodex-3 microcarriers at different cell to bead ratios. Ratios shown include 5:1 (A), 50:1 (B), and 200:1 (C, D).

3.2 Comparison of Spheroid and Microbead Assays

3.2.1 Outgrowth Quantifications

To begin characterizing and comparing the spheroid and microbead assays, various aspects of angiogenesis were examined. These included average total outgrowth, number of strands, strand length, cells per strand, and degree of branching. Spheroids (1200 HUVECs) or microbeads (50:1 HUVEC:bead) were embedded in a 3 mg/ml collagen matrix and allowed to grow in endothelial growth medium 2 (EGM-2) for 24 hours. Twenty-four hours is a common end-point for investigation of angiogenic growth [57-62]. Upon quantification in ImageJ, the spheroid assay was found to demonstrate significantly increased outgrowth, number of strands, strand length, cells per strand, and degree of branching relative to the microbead assay (Figure 3B-F). Total outgrowth was quantified by subtracting the area of the core from the area of the entire spheroid or microbead and dividing by the area of the core. This normalized the outgrowth to the exact core size of the spheroid or microbead to account for any possible variation. The number of cells per strand was determined by counting the number of nuclei in each strand, as indicated by the DAPI stain. The degree of branching was determined by dividing the number of strands that appeared to have split into two sprouts by the total number of strands. Branching is an important part of angiogenesis because it ensures that the neovascularization sufficiently perfuses the target tissue [63].

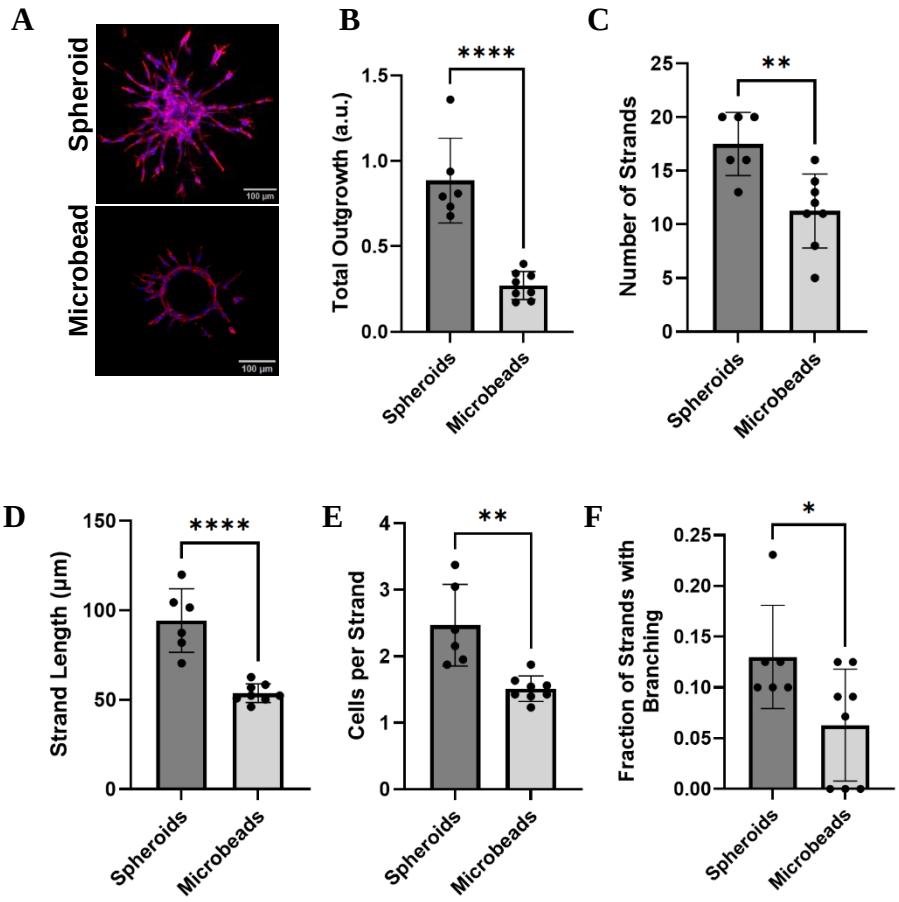

Figure 3. Comparison of spheroids and microbeads after 24 hours of growth in 3 mg/ml collagen. (A) Representative images of spheroids and microbeads stained with TexasRed-X Phalloidin (red) and DAPI (blue) are shown. Average total outgrowth (B), number of strands (C), strand length (D), cells per strand (E), and degree of branching (F) were quantified using ImageJ. Statistical significances were determined using an unpaired t-test. Error bars indicate standard deviation. N=3, n=6, 8 for spheroids and microbeads, respectively.

3.2.2 Effects of Matrix Density

Next, the effects of matrix density on angiogenic outgrowth from both assays were determined. Spheroids (1200 HUVECs) and microbeads (50:1 HUVEC:bead) were embedded in 1.5 and 4.5 mg/ml collagen and allowed to grow in EGM-2 for twenty four hours. Outgrowth was quantified in the same way as above and then normalized to the respective growth in 3.0 mg/ml to allow for a quantitative comparison of the two assays. When the collagen density decreased from 3 mg/ml to 1.5 mg/ml, the spheroid and microbead assays showed a 34.55% and 31.86% increase in outgrowth, respectively (Figure 4C). Conversely, when the collagen density increased from 3 mg/ml to 4.5 mg/ml, the spheroid and microbead assays showed a 29.30% and 24.72% decrease in outgrowth, respectively (Figure 4C). Both models showed increased outgrowth when collagen

density decreased and decreased outgrowth when collagen density increased (Figure 4B). This was expected and is consistent with the trends from literature previously discussed [37-40]. In both cases, the microbead assay appeared to be slightly less responsive to changes in matrix density than the spheroid assay, but no significant difference was found.

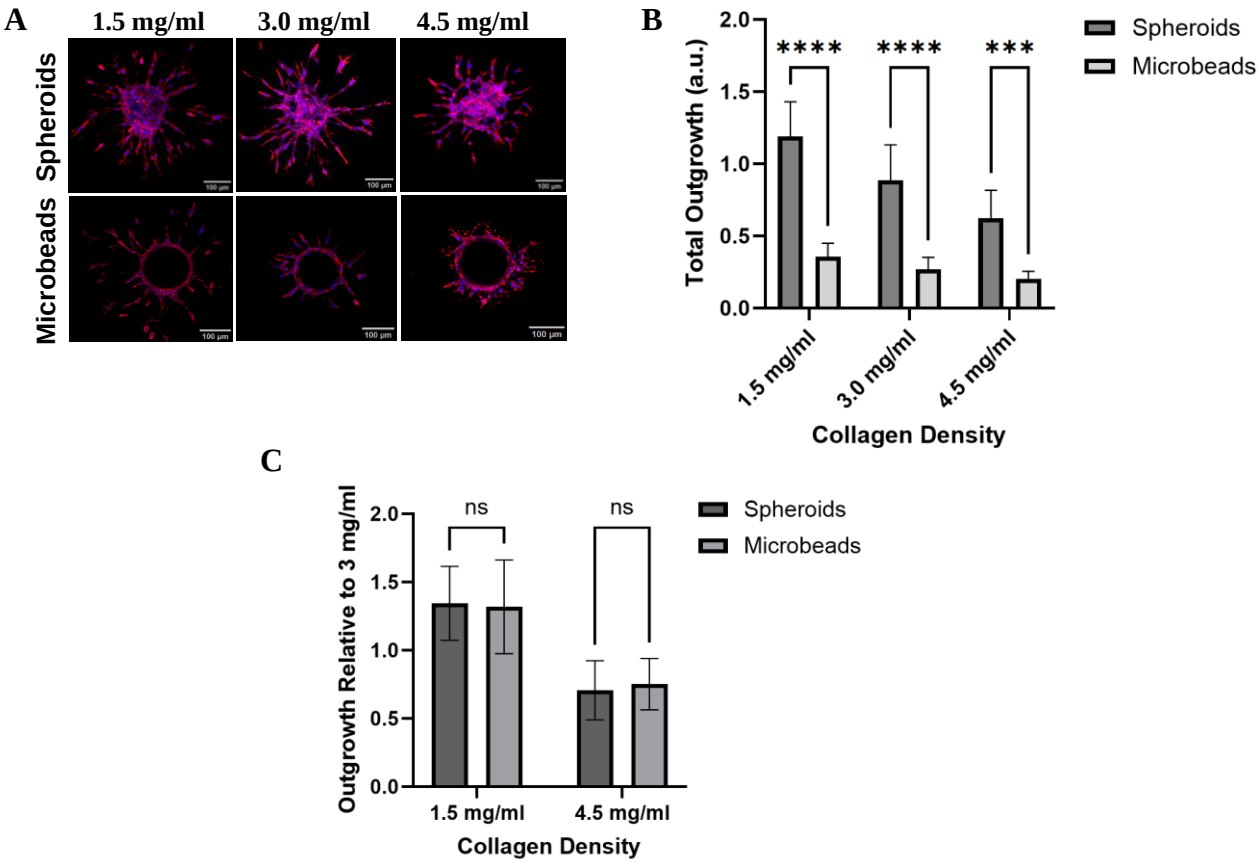

Figure 4. Effect of collagen density on angiogenic outgrowth in spheroid and microbead assays. (A) Representative images of spheroid and microbead growth after 24 hours in 1.5, 3.0, and 4.5 mg/ml collagen. (B) Spheroid and microbead outgrowth in 1.5, 3.0, and 4.5 mg/ml collagen. (C) Spheroid and microbead outgrowth in 1.5 and 4.5 mg/ml collagen, relative to average outgrowth in 3 mg/ml collagen. Statistical significances were determined using an unpaired t-test. Error bars indicate standard deviation. For both spheroids and microbeads, n=8, 7 for 1.5 mg/ml and 4.5 mg/ml, respectively.

3.2.3 Strand Metabolism

The relative levels of metabolic activity along the angiogenic strands produced by the spheroid and microbead assays were then investigated. Because glycolysis is the primary bioenergetic process that drives angiogenesis, evaluating the extent of glucose uptake by endothelial cells provides a measure of the transpiring metabolic activity. Incubation with 2-NBDG, a fluorescent glucose analog, is a common method of determining glucose uptake and

therefore glycolytic activity [64-65]. Spheroids (1200 HUVECs) and microbeads (50:1 HUVEC:bead) were embedded in 3 mg/ml collagen and allowed to grow for 24 hours in EGM-2. The spheroids and microbeads were then incubated with 0.146 mM 2-NBDG in EGM-2 and allowed to grow for another 24 hours. The resulting signal intensity along the middle of the generated sprouts was measured. Signal intensity was measured from the tip of the strand to the core of the spheroid or microbead. Overlapping strands were not included because of the possibility of signal summation artifacts. The signal intensities for each strand were normalized to the maximum and minimum values, so that the positions on the strand with the highest and lowest signal intensities were assigned a value of one and zero, respectively. All other values were scaled accordingly. Normalizing the signal intensities in this way provided a measure of the levels of 2-NBDG uptake of each position on the strand relative to the entire length of the strand and allowed for a quantitative comparison between the two assays. These normalized values were computed for all distances from the tip of the sprout in 0.6252 micron increments for all strands. The normalized values were averaged for each distance from the tip of the strand to compare the relative glucose uptake levels along angiogenic sprouts generated by both assays.

Both assays exhibited increased 2-NBDG uptake towards the tip of the strand relative to the rest of the strand (Figure 5B). They both show a drop in 2-NBDG uptake around 15-20 microns (Figure 5B). The average size of a single HUVEC is 17 microns, so this likely corresponds with the relative location on the strand where the transition from the tip cell to the stalk cell begins [66]. This suggests that the tip cells displayed increased metabolic activity relative to the proceeding stalk cells, which is expected and consistent with known angiogenic trends [48-51]. Spheroids and microbeads displayed very similar maximum average signals of 0.6324 and 0.6327 at 6.88 and 5.00 microns from the tip of the strands, respectively (Figure 5B). However, microbead strands demonstrated a minimum average signal of 0.1861 at 29.38 microns, which is considerably less than the minimum average signal of the spheroid strands, 0.3317 at 44.39 microns (Figure 5B). This suggests that the difference between tip cell metabolism and stalk cell metabolism could be greater in the microbead assay than the spheroid assay. Both assays also demonstrate relatively low 2-NBDG levels at the extremity of the strand (0 microns) (Figure 5B). This can likely be attributed to the dynamic filopodia that are associated with the leading edge of endothelial tip cells. 2-NBDG typically localizes to the cytoplasm of cells [67]. The cytoplasmic volumes of filopodia

are relatively low due to filopodia structure, so filopodia would inherently exhibit low levels of 2-NBDG.

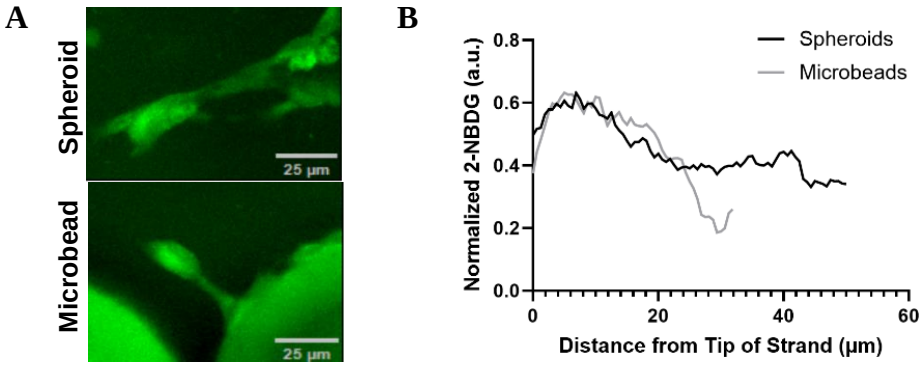

Figure 5. Average 2-NBDG uptake along spheroid sprouts and microbead sprouts after 48 hours of growth. Signal intensity values were normalized to the minimum and maximum values of each strand to provide a measure of the relative levels of 2-NBDG uptake at each position along the strand with respect to the strand as a whole. N=3, n>25, 10 for spheroid and microbead sprouts, respectively.

3.3 Effect of Matrix Density on Tip/Stalk Metabolism

We next investigated the impact of collagen density on the metabolic activity of endothelial tip and stalk cells. We chose to use the spheroid sprouting assay for this analysis because of the increased angiogenic output and strand lengths relative to the microbead assay. To do this, spheroids (1200 HUVECs) were embedded in 1.5, 3, 4.5 mg/ml collagen and allowed to grow for 24 hours in EGM-2. They were then incubated with 0.146 mM 2-NBDG in EGM-2 and allowed to grow for another 24 hours. The signal intensities along the strands were then determined in the same way as above.

All three densities generated strands that exhibited an increase in 2-NBDG uptake towards the tip of the strands relative to the rest of the strand (Figure 6A). For subsequent analysis, the first 20 microns were considered to represent the tip cell, and the next 20 microns were considered to represent the first stalk cell, in accordance with the average HUVEC size [66]. To compare the differences in relative tip and stalk 2-NBDG uptake along strands in the different collagen densities, the 2-NBDG measurements for the first and second set of 20 microns from the sprout tip were averaged and compared. Tip cells demonstrated significantly increased 2-NBDG uptake relative to their proceeding stalk cells in sprouts produced by all three densities (Figure 6C). However, no significant difference in tip-stalk glucose uptake was found between collagen densities.

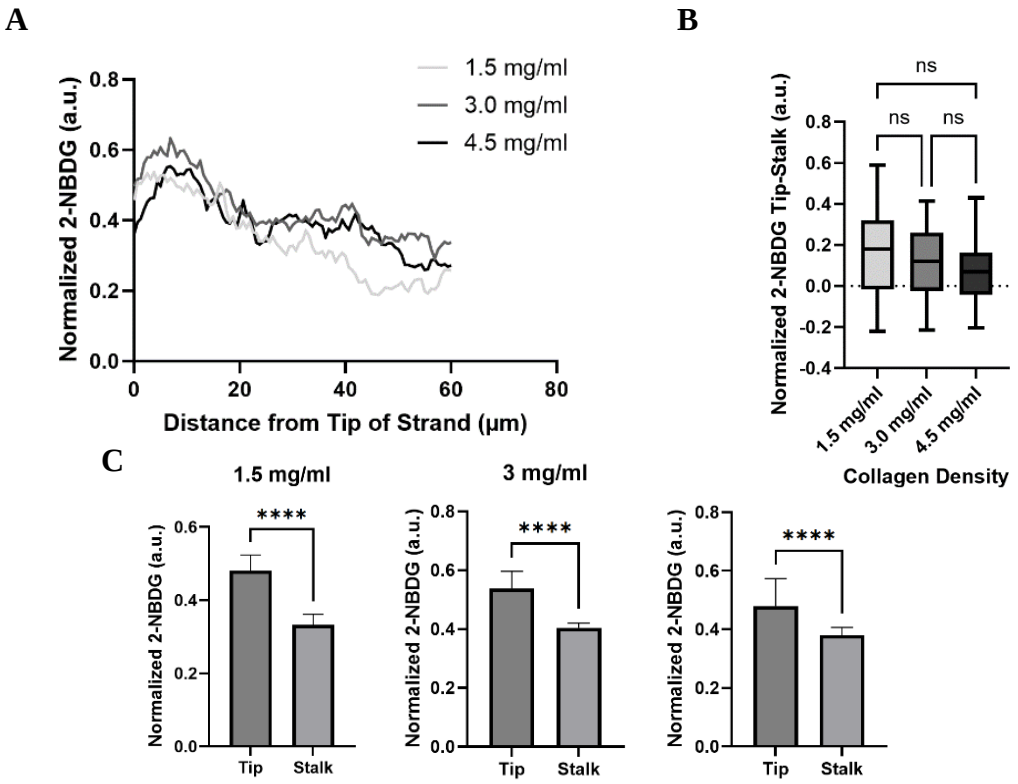

Figure 6. (A) Average 2-NBDG uptake along spheroid sprouts after 48 hours of growth in 1.3, 3.0, and 4.5 mg/ml collagen. Signal intensity values were normalized to the minimum and maximum values of each strand. This provided a measure of the relative levels of 2-NBDG uptake at each position along the strand with respect to the strand as a whole. (B) Relative levels of 2-NBDG uptake were compared between densities for tip and stalk cells. (C) Differences in tip and stalk 2-NBDG uptake in different collagen densities. Statistical significances were determined using an unpaired t-test (C) or a one-way ANOVA followed by Tukey's multiple comparisons test (B). Error bars indicate standard deviation. N=3, n>23, 26, 32 for 1.5, 3.0, and 4.5 mg/ml, respectively.

3.4 Generation of MMP-14 KO HUVECs

Lastly, we investigated the generation of a line of HUVECs with an MMP-14 knockout for future analysis of the role of MMP-14 in tip and stalk endothelial cells. HUVECs are primary cells and known for being difficult to transfect because of their limited viability in non-optimal conditions [68]. We attempted to transfect HUVECs with single guide RNA for a MMP-14 knockout using electroporation and a CRISPR/cas9 system. RNP complexes containing Cas9 and the sgRNA were added to HUVECs in electroporation buffer. The cells were then subjected to an exponential decay pulse of 120 V and 950 µF and allowed to recover for several days. About three days into the recovery phase, the HUVECs began to die, resulting in failed transfection.

Chapter 4
Discussion

4.1 Comparison of Spheroid and Microbead Assays

In this study, the spheroid and microbead models of angiogenesis were characterized and compared. Because these two *in vitro* models are incredibly similar, determining their angiogenic properties and slight differences could inform one's decision of which model to use for their desired purposes. The results of this study indicate that the spheroid sprouting assay produced increased angiogenic output relative to the microbead assay, as shown through increased total outgrowth, number of strands, strand length, and cells/strand. One potential explanation for this could be that the HUVECs in the core of spheroids secrete growth factors, resulting in an increased amount of pro-angiogenic stimuli relative to microbeads.

These results suggest that if one's goal is solely to generate large quantities of sprouts, the spheroid assay would be more beneficial. Additionally, the longer strands with more cells that resulted from the spheroid assay could provide more information about cell-cell interactions that occur during angiogenesis than the shorter and frequently unicellular sprouts that resulted from the microbead assay. The spheroid assay also resulted in increased branching compared to the microbead assay. Angiogenic branching is essential to ensure that the developing blood vessel network completely perfuses the target area [67]. However, an advantage of the microbead assay was the ease of quantification. The clearly defined core and the decreased angiogenic output resulted in straightforward evaluation of its characteristics. To potentially increase the angiogenic output of the microbead assay, one could increase the allotted time for growth after embedding in collagen. While the increased duration of the assay would not be ideal, this could result in improved outgrowth and longer strands for a more developed model, although there is a potential risk of increased cell fragmentation off the strands.

Next, the effect of matrix density on angiogenic growth was investigated because of the high levels of interaction between neovessels and the ECM. The results indicated an inverse relationship between outgrowth and collagen density in both models. This is in accordance with existing studies [37-40]. The microbead assay appeared to be slightly less responsive to both increased and decreased collagen densities than the spheroid assay, although these differences were not significant. However, if the difference in collagen density was greater, it is possible that a significant difference in responsivity could be found between the two models.

The relative metabolic activity throughout angiogenic strands was then investigated and compared. Both assays exhibited higher metabolic activity at the tips of the strands than the stalk, as indicated by 2-NBDG uptake. Because a known characteristic of endothelial tip cells is increased metabolism relative to stalk cells to support cell migration, this was expected [48-50]. The increase in metabolic activity between tip cells and the corresponding stalk cells in their sprout appeared to be somewhat greater in microbead strands than spheroid strands. However, the short length of the microbead strands resulted in a limited amount of information on the glucose uptake levels of stalk cells, so this claim may not be well supported. In order to better characterize the metabolic patterns between tip and stalk cells in microbead sprouts, the length of the strands, and therefore the number of cells per strand, would need to be increased. This could possibly be done by an increased growth period after embedding in collagen, as stated above.

For subsequent investigation of the effects of matrix density on endothelial cell metabolism during angiogenesis, one of these models had to be selected. We chose to move forward with the spheroid sprouting assay instead of the microbead assay. We chose the spheroid assay for several reasons. First, the increased angiogenic output (number and length of strands) would simply increase the amount of data that is able to be collected from one iteration of the assay. This would save both time and materials during the course of investigation. The longer sprouts produced by the spheroid assay were also ideal for evaluation of metabolic gradients along angiogenic strands. Because many of the microbead sprouts were unicellular and differences in angiogenic metabolism are primarily determined by endothelial cell phenotype, longer strands with multiple cells would be more advantageous for this analysis. Additionally, spheroids were demonstrated to be somewhat more responsive to matrix density than microbeads. This suggested that the spheroid assay could potentially highlight the effects of density changes on metabolism that could be less apparent in the microbead assay. Although it is possible that the difference in tip and stalk metabolism is greater in the microbead assay than the spheroid assay, this was not enough to overcome the guaranteed advantages of increased angiogenic output and strand length that are associated with the spheroid assay.

4.2 Effect of Matrix Density on Strand Metabolic Gradients

Using the spheroid sprouting assay, we subsequently investigated the effects of collagen density on the metabolic activity of angiogenic strands. Spheroids were allowed to grow for 48 hours in 1.5, 3.0, and 4.5 mg/ml collagen and the resulting levels of glucose uptake were

determined with fluorescent 2-NBDG. Because glycolysis is the primary bioenergetic process that drives angiogenesis, glucose uptake acted as a measure of overall cell metabolism. Sprouts from all densities had increased average glucose uptake towards the tip of the strand, and tip cells had significantly increased average glucose uptake relative to their corresponding stalk cells. Because a known characteristic of tip cells is increased cell metabolism relative to stalk cells, this was expected.

Next, we compared the relative levels of glucose uptake along strands in tip and stalk cells from the different densities. Denser matrices provide a larger barrier to cell migration and therefore require increased energy generation to overcome this burden [69]. Tip cells are the main drivers of cell migration during angiogenesis and have been shown to exhibit increased metabolic activity in denser matrices [49]. Stalk cells have been reported to interact with the extracellular matrix to a smaller degree than tip cells and are thought to have a minimal role in cell migration, so we hypothesized that stalk cell metabolism would not change with the matrix density. However, we found that there was no significant difference between tip-stalk metabolic activity in the different collagen densities, which suggests that both tip and stalk metabolism increased with collagen density.

The results of this study indicate that tip cells have increased metabolic activity relative to their stalk cells and that stalk cells could have some ability to adapt their metabolism in different matrix densities. One possible explanation for this could be that stalk cells interact with the extracellular matrix to a higher than previously thought and could even play a larger role in cell migration. It is also possible that the differences in matrix density investigated were too low to produce sufficiently large changes in tip cell metabolism. To further explore potential stalk cell responsivity to matrix changes, future investigations could include a larger range of collagen densities.

4.3 Role of MMP-14 in Leader/Follower Dynamics

We attempted to transfect HUVECs with sgRNA for an MMP-14 KO using electroporation and CRISPR/cas9. The transfection failed, as the HUVECs died during the recovery phase after electroporation. Alternative transfection methods that will be investigated include altered electroporation settings and chemical transfection. Some success with transfecting HUVECs has been reported using electroporation with a square wave pulse instead of exponential decay [70]. Additionally, Lipofectamine LTX has been shown to be somewhat effective [68].

Once a HUVEC line with an MMP-14 KO has been obtained, it could be used for future investigations into tip/stalk dynamics. Currently, the potential role of stalk cells in matrix degradation has been poorly characterized. To examine this, spheroids could be created with both wild-type and KO HUVECs and embedded in a collagen gel to induce angiogenesis. After some growth period, the localization of the KO HUVECs in angiogenic strands could be determined. Because tip cells have been shown to play a large role in matrix degradation, we hypothesize that the ability to facilitate matrix degradation through functional MMP-14 is not required for stalk cell differentiation and is required for tip cell differentiation.

Overall, developing a better understanding of angiogenesis and the distinct relationships of tip and stalk cells with the extracellular matrix is advantageous for a variety of applications. For example, this could inform mechanisms to improve the efficacy of incorporating sufficient vascularization into tissue engineered products, which is a current challenge in the field. Additionally, this could help with the development of anti-cancer therapies. Tumor-induced angiogenesis is essential for tumors to continue to grow and metastasize. Understanding how the characteristics of the tumor microenvironment regulate and interact with the specific endothelial cell subtypes during angiogenesis could inform the development of treatments to limit or even completely inhibit tumor growth.

References

1. Grisham, J. (2014, March 13). *What is angiogenesis?*. Memorial Sloan Kettering Cancer Center. https://www.mskcc.org/news/what-angiogenesis
2. Adair, T. H. (2010, January 1). *Overview of angiogenesis*. Angiogenesis. https://www.ncbi.nlm.nih.gov/books/NBK53238/
3. Hillen, F., & Griffioen, A. W. (2007). Tumour vascularization: Sprouting angiogenesis and beyond. *Cancer and Metastasis Reviews*, *26*(3–4), 489–502. https://doi.org/10.1007/s10555-007-9094-7
4. *Angiogenesis inhibitors*. National Cancer Institute. (2018). https://www.cancer.gov/about-cancer/treatment/types/immunotherapy/angiogenesis-inhibitors-fact-sheet#:~:text=Angiogenesis%20is%20the%20formation%20of,chemical%20signals%20in%20the%20body
5. Tonnesen, M. G., Feng, X., & Clark, R. A. F. (2000). Angiogenesis in wound healing. *Journal of Investigative Dermatology Symposium Proceedings*, *5*(1), 40–46. https://doi.org/10.1046/j.1087-0024.2000.00014.x
6. Veith, A. P., Henderson, K., Spencer, A., Sligar, A. D., & Baker, A. B. (2019). Therapeutic strategies for enhancing angiogenesis in wound healing. *Advanced Drug Delivery Reviews*, *146*, 97–125. https://doi.org/10.1016/j.addr.2018.09.010
7. Kumar, P., Kumar, S., Udupa, E. P., Kumar, U., Rao, P., & Honnegowda, T. (2015b). Role of angiogenesis and angiogenic factors in acute and chronic wound healing. *Plastic and Aesthetic Research*, *2*(5), 243. https://doi.org/10.4103/2347-9264.165438
8. Muthukkaruppan, V. R., Kubai, L., & Aurebach, R. (1982). Tumor-induced neovascularization in the mouse eye23. *JNCI: Journal of the National Cancer Institute*. https://doi.org/10.1093/jnci/69.3.699
9. Holmgren, L., O'Reilly, M. S., & Folkman, J. (1995). Dormancy of micrometastases: Balanced proliferation and apoptosis in the presence of angiogenesis suppression. *Nature Medicine*, *1*(2), 149–153. https://doi.org/10.1038/nm0295-149
10. Muz, B., de la Puente, P., Azab, F., & Azab, A. K. (2015). The role of hypoxia in cancer progression, angiogenesis, metastasis, and resistance to therapy. *Hypoxia*, 83. https://doi.org/10.2147/hp.s93413
11. Gupta, M. K., & Qin, R.-Y. (2003). Mechanism and its regulation of tumor-induced angiogenesis. *World Journal of Gastroenterology*, *9*(6), 1144. https://doi.org/10.3748/wjg.v9.i6.1144
12. Nishida, N., Yano, H., Nishida, T., Kamura, T., & Kojiro, M. (2006). Angiogenesis in cancer. *Vascular Health and Risk Management*, *2*(3), 213–219. https://doi.org/10.2147/vhrm.2006.2.3.213
13. U.S. Department of Health and Human Services. (n.d.). *Tissue engineering and regenerative medicine*. National Institute of Biomedical Imaging and Bioengineering. https://www.nibib.nih.gov/science-education/science-topics/tissue-engineering-and-regenerative-medicine
14. Jahani, M., Rezazadeh, D., Mohammadi, P., Abdolmaleki, A., Norooznezhad, A., & Mansouri, K. (2020). Regenerative Medicine and angiogenesis; challenges and opportunities. *Advanced Pharmaceutical Bulletin*, *10*(4), 490–501. https://doi.org/10.34172/apb.2020.061

15. Chandra, P., & Atala, A. (2019). Engineering blood vessels and vascularized tissues: Technology trends and potential clinical applications. *Clinical Science*, *133*(9), 1115–1135. https://doi.org/10.1042/cs20180155
16. Mastrullo, V., Cathery, W., Velliou, E., Madeddu, P., & Campagnolo, P. (2020, February 26). *Angiogenesis in tissue engineering: As nature intended?*. Frontiers. https://www.frontiersin.org/articles/10.3389/fbioe.2020.00188/full
17. Blacher, S., Erpicum, C., Lenoir, B., Paupert, J., Moraes, G., Ormenese, S., Bullinger, E., & Noel, A. (2014). Cell invasion in the spheroid sprouting assay: A spatial organisation analysis adaptable to cell behaviour. *PLoS ONE*, *9*(5). https://doi.org/10.1371/journal.pone.0097019
18. Tetzlaff, F., & Fischer, A. (2018). Human endothelial cell spheroid-based sprouting angiogenesis assay in collagen. *BIO-PROTOCOL*, *8*(17). https://doi.org/10.21769/bioprotoc.2995
19. *Microcarrier*. Microcarrier - an overview | ScienceDirect Topics. (n.d.). https://www.sciencedirect.com/topics/pharmacology-toxicology-and-pharmaceutical-science/microcarrier#:~:text=Microcarriers%20provide%20anchorage%20or%20an,cellulose%2C%20plastic%2C%20or%20glass
20. Nehls, V., & Drenckhahn, D. (1995). A novel, microcarrier-based in vitro assay for rapid and reliable quantification of three-dimensional cell migration and angiogenesis. *Microvascular Research*, *50*(3), 311–322. https://doi.org/10.1006/mvre.1995.1061
21. Bellacen, K., & Lewis, E. C. (2009). Aortic Ring Assay. *Journal of Visualized Experiments*, (33). https://doi.org/10.3791/1564
22. Nicosia, R. F. (2009). The aortic ring model of angiogenesis: A quarter century of search and Discovery. *Journal of Cellular and Molecular Medicine*, *13*(10), 4113–4136. https://doi.org/10.1111/j.1582-4934.2009.00891.x
23. Ribatti, D. (2011). Chicken chorioallantoic membrane angiogenesis model. *Methods in Molecular Biology*, 47–57. https://doi.org/10.1007/978-1-61779-523-7_5
24. Storgard, C., Mikolon, D., & Stupack, D. G. *Angiogenesis assays in the chick cam*. SpringerLink. https://link.springer.com/protocol/10.1385/1-59259-860-9:123
25. Zarkada, G., Howard, J. P., Xiao, X., Park, H., Bizou, M., Leclerc, S., Künzel, S. E., Boisseau, B., Li, J., Cagnone, G., Joyal, J. S., Andelfinger, G., Eichmann, A., & Dubrac, A. (2021). Specialized endothelial tip cells guide neuroretina vascularization and blood-retina-barrier formation. *Developmental Cell*, *56*(15). https://doi.org/10.1016/j.devcel.2021.06.021
26. Blanco, R., & Gerhardt, H. (2012). VEGF and notch in tip and stalk cell selection. *Cold Spring Harbor Perspectives in Medicine*, *3*(1). https://doi.org/10.1101/cshperspect.a006569
27. Gerhardt, H., Golding, M., Fruttiger, M., Ruhrberg, C., Lundkvist, A., Abramsson, A., Jeltsch, M., Mitchell, C., Alitalo, K., Shima, D., & Betsholtz, C. (2003). VEGF guides angiogenic sprouting utilizing endothelial tip cell filopodia. *The Journal of Cell Biology*, *161*(6), 1163–1177. https://doi.org/10.1083/jcb.200302047
28. Dong, Y., Alonso, F., Jahjah, T., Fremaux, I., & Génot, E. (n.d.). *Angiogenesis invasion assay to study endothelial cell invasion and sprouting behavior*. SpringerLink. https://link.springer.com/protocol/10.1007/978-1-0716-2887-4_20
29. Chen, W., Xia, P., Wang, H., Tu, J., Liang, X., Zhang, X., & Li, L. (2019). The endothelial tip-stalk cell selection and shuffling during angiogenesis. *Journal of Cell*

Communication and Signaling, *13*(3), 291–301. https://doi.org/10.1007/s12079-019-00511-z
30. Rundhaug, J. E. (2007). Matrix metalloproteinases and angiogenesis. *Journal of Cellular and Molecular Medicine*, *9*(2), 267–285. https://doi.org/10.1111/j.1582-4934.2005.tb00355.x
31. Stetler-Stevenson, W. G. (1999). Matrix metalloproteinases in angiogenesis: A moving target for therapeutic intervention. *Journal of Clinical Investigation*, *103*(9), 1237–1241. https://doi.org/10.1172/jci6870
32. *MMP14*. MMP14 - an overview | ScienceDirect Topics. (n.d.). https://www.sciencedirect.com/topics/biochemistry-genetics-and-molecular-biology/mmp14
33. Jabłońska-Trypuć, A., Matejczyk, M., & Rosochacki, S. (2016). Matrix metalloproteinases (mmps), the main extracellular matrix (ECM) enzymes in collagen degradation, as a target for anticancer drugs. *Journal of Enzyme Inhibition and Medicinal Chemistry*, *31*, 177–183. https://doi.org/10.3109/14756366.2016.1161620
34. Quintero-Fabián, S., Arreola, R., Becerril-Villanueva, E., Torres-Romero, J. C., Arana-Argáez, V., Lara-Riegos, J., Ramírez-Camacho, M. A., & Alvarez-Sánchez, M. E. (2019). Role of matrix metalloproteinases in angiogenesis and cancer. *Frontiers in Oncology*, *9*. https://doi.org/10.3389/fonc.2019.01370
35. Tranqui, L., & Tracqui, P. (2000). Mechanical signalling and angiogenesis. the integration of cell–extracellular matrix couplings. *Comptes Rendus de l'Académie Des Sciences - Series III - Sciences de La Vie*, *323*(1), 31–47. https://doi.org/10.1016/s0764-4469(00)00110-4
36. Vernon, R. B., & Sage, E. H. (1996). Contraction of fibrillar type I collagen by endothelial cells: A study in vitro. *Journal of Cellular Biochemistry*, *60*(2), 185–197. https://doi.org/10.1002/(sici)1097-4644(19960201)60:2<185::aid-jcb3>3.0.co;2-t
37. Edgar, L. T., Underwood, C. J., Guilkey, J. E., Hoying, J. B., & Weiss, J. A. (2014). Extracellular matrix density regulates the rate of Neovessel growth and branching in sprouting angiogenesis. *PLoS ONE*, *9*(1). https://doi.org/10.1371/journal.pone.0085178
38. Ghajar, C. M., Chen, X., Harris, J. W., Suresh, V., Hughes, C. C. W., Jeon, N. L., Putnam, A. J., & George, S. C. (2008). The effect of matrix density on the regulation of 3-D capillary morphogenesis. *Biophysical Journal*, *94*(5), 1930–1941. https://doi.org/10.1529/biophysj.107.120774
39. Kniazeva, E., & Putnam, A. J. (2009). Endothelial cell traction and ECM density influence both capillary morphogenesis and maintenance in 3-D. *American Journal of Physiology-Cell Physiology*, *297*(1). https://doi.org/10.1152/ajpcell.00018.2009
40. Sieminski, A. L., Hebbel, R. P., & Gooch, K. J. (2004). The relative magnitudes of endothelial force generation and matrix stiffness modulate capillary morphogenesis in vitro. *Experimental Cell Research*, *297*(2), 574–584. https://doi.org/10.1016/j.yexcr.2004.03.035
41. *Cell metabolism*. Cell Metabolism - an overview | ScienceDirect Topics. (n.d.). https://www.sciencedirect.com/topics/medicine-and-dentistry/cell-metabolism#:~:text=Cellular%20metabolism%20is%20comprised%20of,the%20synthesis%20of%20larger%20biomolecules

42. Fraisl, P., Mazzone, M., Schmidt, T., & Carmeliet, P. (2009). Regulation of angiogenesis by oxygen and metabolism. *Developmental Cell*, *16*(2), 167–179. https://doi.org/10.1016/j.devcel.2009.01.003
43. De Bock, K., Georgiadou, M., Schoors, S., Kuchnio, A., Wong, B. W., Cantelmo, A. R., Quaegebeur, A., Ghesquière, B., Cauwenberghs, S., Eelen, G., Phng, L.-K., Betz, I., Tembuyser, B., Brepoels, K., Welti, J., Geudens, I., Segura, I., Cruys, B., Bifari, F., … Carmeliet, P. (2013). Role of PFKFB3-driven glycolysis in vessel sprouting. *Cell*, *154*(3), 651–663. https://doi.org/10.1016/j.cell.2013.06.037
44. Dumas, S. J., García-Caballero, M., & Carmeliet, P. (2020). Metabolic signatures of distinct endothelial phenotypes. *Trends in Endocrinology & Metabolism*, *31*(8), 580–595. https://doi.org/10.1016/j.tem.2020.05.009
45. De Bock, K., Georgiadou, M., Schoors, S., Kuchnio, A., Wong, B. W., Cantelmo, A. R., Quaegebeur, A., Ghesquière, B., Cauwenberghs, S., Eelen, G., Phng, L.-K., Betz, I., Tembuyser, B., Brepoels, K., Welti, J., Geudens, I., Segura, I., Cruys, B., Bifari, F., … Carmeliet, P. (2013a). Role of PFKFB3-driven glycolysis in vessel sprouting. *Cell*, *154*(3), 651–663. https://doi.org/10.1016/j.cell.2013.06.037
46. Buchwald, P. (2011). A local glucose-and oxygen concentration-based insulin secretion model for pancreatic islets. *Theoretical Biology and Medical Modelling*, *8*(1). https://doi.org/10.1186/1742-4682-8-20
47. Real-Hohn, A., Zancan, P., Da Silva, D., Martins, E. R., Salgado, L. T., Mermelstein, C. S., Gomes, A. M. O., & Sola-Penna, M. (2010). Filamentous actin and its associated binding proteins are the stimulatory site for 6-phosphofructo-1-kinase association within the membrane of human erythrocytes. *Biochimie*, *92*(5), 538–544. https://doi.org/10.1016/j.biochi.2010.01.023
48. De Bock, K., Georgiadou, M., & Carmeliet, P. (2013). Role of endothelial cell metabolism in vessel sprouting. *Cell Metabolism*, *18*(5), 634–647. https://doi.org/10.1016/j.cmet.2013.08.001
49. Zanotelli, M. (2019). *Energetic costs regulated by cell mechanics and confinement are predictive of migration path during decision-making.* [Doctoral dissertation, Vanderbilt University]. Vanderbilt University Institutional Repository.
50. Stapor, P., Wang, X., Goveia, J., Moens, S., & Carmeliet, P. (2014). Angiogenesis revisited – role and therapeutic potential of targeting endothelial metabolism. *Journal of Cell Science*. https://doi.org/10.1242/jcs.153908
51. Verdegem, D., Moens, S., Stapor, P., & Carmeliet, P. (2014). Endothelial cell metabolism: Parallels and divergences with cancer cell metabolism. *Cancer & Metabolism*, *2*(1). https://doi.org/10.1186/2049-3002-2-19
52. *Cytodex 3 microcarriers (dry powder)*. Cytiva. (n.d.). https://www.cytivalifesciences.com/en/us/shop/cell-culture-and-fermentation/microcarriers/cytodex-3-microcarriers-dry-powder-p-05925
53. Amoorahim, M., Valipour, E., Hoseinkhani, Z., Mahnam, A., Rezazadeh, D., Ansari, M., Shahlaei, M., Gamizgy, Y. H., Moradi, S., & Mansouri, K. (2020). TSGA10 overexpression inhibits angiogenesis of huvecs: A hif-2α biased perspective. *Microvascular Research*, *128*, 103952. https://doi.org/10.1016/j.mvr.2019.103952
54. Fotticchia, I., Guarnieri, D., Fotticchia, T., Falanga, A. P., Vecchione, R., Giancola, C., & Netti, P. A. (2016). Energetics of ligand-receptor binding affinity on endothelial cells:

AN in vitro model. *Colloids and Surfaces B: Biointerfaces*, *144*, 250–256. https://doi.org/10.1016/j.colsurfb.2016.04.018
55. Samadian, E., Colagar, A. H., Safarzad, M., Asadi, J., & Mansouri, K. (2023). Inhibitory potency of the nettle lectin on neovascularization: A biomolecule for carbohydrate-mediated targeting of angiogenesis. *Molecular Biology Reports*, *50*(5), 4491–4503. https://doi.org/10.1007/s11033-023-08355-y
56. Nakatsu, M. N., Davis, J., & Hughes, C. C. W. (2007). Optimized fibrin gel bead assay for the study of angiogenesis. *Journal of Visualized Experiments*, (3). https://doi.org/10.3791/186
57. Anada, T., Pan, C.-C., Stahl, A., Mori, S., Fukuda, J., Suzuki, O., & Yang, Y. (2019). Vascularized bone-mimetic hydrogel constructs by 3D bioprinting to promote osteogenesis and angiogenesis. *International Journal of Molecular Sciences*, *20*(5), 1096. https://doi.org/10.3390/ijms20051096
58. Fedele, C., De Gregorio, M., Netti, P. A., Cavalli, S., & Attanasio, C. (2017). Azopolymer photopatterning for directional control of angiogenesis. *Acta Biomaterialia*, *63*, 317–325. https://doi.org/10.1016/j.actbio.2017.09.022
59. Weber, H., Claffey, J., Hogan, M., Pampillón, C., & Tacke, M. (2008). Analyses of titanocenes in the spheroid-based cellular angiogenesis assay. *Toxicology in Vitro*, *22*(2), 531–534. https://doi.org/10.1016/j.tiv.2007.09.014
60. Du, K., Zhao, C., Wang, L., Wang, Y., Zhang, K.-Z., Shen, X.-Y., Sun, H.-X., Gao, W., & Lu, X. (2019). Mir-191 inhibit angiogenesis after acute ischemic stroke targeting VEZF1. *Aging*, *11*(9), 2762–2786. https://doi.org/10.18632/aging.101948
61. Peng, Y., Wang, Y., Tang, N., Sun, D., Lan, Y., Yu, Z., Zhao, X., Feng, L., Zhang, B., Jin, L., Yu, F., Ma, X., & Lv, C. (2018). Andrographolide inhibits breast cancer through suppressing COX-2 expression and angiogenesis via inactivation of p300 signaling and VEGF pathway. *Journal of Experimental & Clinical Cancer Research*, *37*(1). https://doi.org/10.1186/s13046-018-0926-9
62. Zhang, Y., Liu, J., Zou, T., Qi, Y., Yi, B., Dissanayaka, W. L., & Zhang, C. (2021). DPSCs treated by TGF-β1 regulate angiogenic sprouting of three-dimensionally co-cultured HUVECS and dpscs through VEGF-ang-tie2 signaling. *Stem Cell Research & Therapy*, *12*(1). https://doi.org/10.1186/s13287-021-02349-y
63. Red-Horse, K., & Siekmann, A. F. (2019). Veins and arteries build hierarchical branching patterns differently: Bottom-up versus Top-Down. *BioEssays*, *41*(3). https://doi.org/10.1002/bies.201800198
64. Zou, C., Wang, Y., & Shen, Z. (2005). 2-NBDG as a fluorescent indicator for direct glucose uptake measurement. *Journal of Biochemical and Biophysical Methods*, *64*(3), 207–215. https://doi.org/10.1016/j.jbbm.2005.08.001
65. Jin, J., Qiu, S., Wang, P., Liang, X., Huang, F., Wu, H., Zhang, B., Zhang, W., Tian, X., Xu, R., Shi, H., & Wu, X. (2019). Cardamonin inhibits breast cancer growth by repressing hif-1α-dependent metabolic reprogramming. *Journal of Experimental & Clinical Cancer Research*, *38*(1). https://doi.org/10.1186/s13046-019-1351-4
66. *Size of HUVEC (human umbilical vein endothelial cell)*. Size of HUVEC (human umbilical vein endotheli - Human Homo sapiens - BNID 108923. (n.d.). https://bionumbers.hms.harvard.edu/bionumber.aspx?s=n&v=0&id=108923
67. ScienceDirect. (n.d.-a). *Filopodia*. Filopodia - an overview. https://www.sciencedirect.com/topics/agricultural-and-biological-

sciences/filopodia#:~:text=Filopodia%20express%20growth%20factor%20and,Mattila%20and%20Lappalainen%2C%202008).
68. Hunt, M. A., Currie, M. J., Robinson, B. A., & Dachs, G. U. (2010). Optimizing transfection of primary human umbilical vein endothelial cells using commercially available chemical transfection reagents. *Journal of biomolecular techniques : JBT*, *21*(2), 66–72.
69. Gonçalves, I. G., & Garcia-Aznar, J. M. (2021). Extracellular matrix density regulates the formation of tumour spheroids through cell migration. *PLOS Computational Biology*, *17*(2). https://doi.org/10.1371/journal.pcbi.1008764
70. Jordan, E. T., Collins, M., Terefe, J., Ugozzoli, L., & Rubio, T. (2008). Optimizing electroporation conditions in primary and other difficult-to-transfect cells. *Journal of biomolecular techniques : JBT*, *19*(5), 328–334.

APPENDIX

Protocol for HUVEC attachment to Cytodex-3 Microcarriers and Embedding in Collagen

1. Hydrate 10 mg Cytodex-3 Microcarriers in 1X PBS in a glass vial overnight
    i. 10 mg = 30,000 microbeads
2. Cover top of vial with aluminum foil and sterilize microbeads with a 30 minute liquid autoclave cycle at 121 °C and allow to cool off for 30 minutes
3. In biosafety cabinet, wash microbeads two times with 5 ml PBS
    i. Wait ~five minutes for beads to drop to bottom of vial before aspirating PBS
4. Hydrate microbeads in 5 ml EGM-2 for 5 minutes and transfer to 15 ml tube
    i. The transfer to the 15 ml tube is easier if done before beads drop to bottom of vial
5. Aspirate media except for ~1 ml and add 1.5 million cells
6. Add 4 ml EGM-2 and incubate at 37 °C and 5% CO_2 for four hours on orbital shaker at speed 4 (approximately 2 rotations/second)
7. Transfer to T25 flask and incubate at 37 °C and 5% CO_2 for sixteen hours, still on the orbital shaker at speed 4
8. Transfer microbeads to 15 ml tube. Wash flask with 5 ml warm EGM-2 and place in same 15 ml tube
9. Wait ~5 minutes for microbeads to fall to bottom of tube
10. Place 40 µl microbeads into premade collage solution (1.1 ml) with wide bore pipet tip
11. Add 11 µl 1 N NaOH and mix until homogenous
12. Pipette 500 µl into two wells of a sterile, 24 well plate
13. Place in incubator and allow to polymerize for 45 minutes
14. Place 1 ml EGM-2 on top of each well and incubate for desired growth period

*This protocol is for a 50:1 cell:bead ratio, which I found to be effective. However, the cell:bead ratio can be altered by changing the amount of Cytodex-3 or cells.